Chemical Science

EDGE ARTICLE

View Article Online
View Journal | View Issue

Cite this: *Chem. Sci.*, 2015, **6**, 714

Chiral tether-mediated stabilization and helix-sense control of complementary metallo-double helices†

Miki Horie,[a] Naoki Ousaka,[b] Daisuke Taura[a] and Eiji Yashima*[a]

Received 30th July 2014
Accepted 10th September 2014

DOI: 10.1039/c4sc02275k

www.rsc.org/chemicalscience

A series of novel Pt^{II}-linked double helices were prepared by inter- or intrastrand ligand-exchange reactions of the complementary duplexes composed of chiral or achiral amidine dimer and achiral carboxylic acid dimer strands joined by *trans*-Pt^{II}–acetylide complexes with PPh_3 ligands using chiral and achiral chelating diphosphines. The structure and stability of the Pt^{II}-linked double helices were highly dependent on the diphosphine structures. An interstrand ligand exchange took place with chiral and achiral 1,3-diphosphine-based ligands, resulting in *trans*-Pt^{II}-bridged double helices, whose helical structures were quite stable even in dimethyl sulfoxide (DMSO) due to the interstrand cross-link, whereas a 1,2-diphosphine-based ligand produced non-cross-linked *cis*-Pt^{II}-linked duplexes, resulting from an intrastrand ligand-exchange that readily dissociated into single strands in DMSO. When enantiopure 1,3-diphosphine-based ligands were used, the resulting *trans*-Pt^{II}-bridged double helices adopted a preferred-handed helical sense biased by the chirality of the bridged diphosphines. Interestingly, the interstrand ligand exchange with racemic 1,3-diphosphine toward an optically-active Pt^{II}-linked duplex, composed of chiral amidine and achiral carboxylic acid strands, was found to proceed in a diastereoselective manner, thus forming complete homochiral *trans*-Pt^{II}-bridged double helices *via* a unique chiral self-sorting.

Introduction

Biological helices, such as double-helical DNA and α-helical peptides, have prompted a number of chemists to construct artificial single- and double-stranded helical polymers[1] and oligomers (foldamers)[2] not only due to their unique structures, but also to their sophisticated functions. Currently, a wide variety of single-stranded helices have been synthesized,[1,2] which enable us to rationally design a single-helical structure from its primary sequence, although it remains a great challenge to create a new structural motif for double-helical structures.[3] However, DNA analogues (peptide nucleic acids, PNAs)[4] and double-stranded helicates are known to intertwine to form double helices assisted by hydrogen bonds and metal-directed coordination, respectively.[3a,b,d,5] A new class of double-stranded helices has recently been developed by Lehn, Huc and co-workers[2c,j,6] that mainly rely on multiple hydrogen bonds between the strands and/or interstrand aromatic–aromatic interactions,[6,7] the stability of which strongly depends on the type of solvent (polar or non-polar)[6b] and sequence,[6d] except for the hydrophobic-driven double helices in water.[8]

It is well-known that intramolecular cross-linking stabilizes a helical conformation of single-stranded helical polymers,[9a,b] foldamers,[9c–f] and oligopeptides,[10] thus leading to the development of smart chiral materials and biologically active materials. The interstrand cross-linking of DNA that reinforces its double-helical structure was also reported to have applications for clinical use.[11] However, to the best of our knowledge, there is at least one precedent of a synthetic double helix whose helical conformation was significantly stabilized as a result of interstrand cross-linking.[12]

Recently, we have developed a versatile method to construct a series of complementary double helices by utilizing amidinium–carboxylate salt bridges that possess high stability and well-defined directionality along their N^+–H···O^- lines, thereby enabling the intertwining of the two complementary molecular strands composed of crescent-shaped rigid *m*-terphenyl backbones.[1e,g,3e,g,i,14] This structural feature has a great advantage such that various types of linker units, such as diacetylene,[14a,e,k] *p*-diethynylbenzene[14f,k] and *trans*-Pt^{II}–acetylide linkages,[12,14b,i,k] can be introduced while maintaining the double-helical structures. In addition, the helical sense and handedness of the double helices are readily controlled by the chiral substituents introduced on the amidine groups,[14] or by using chiral

[a]*Department of Molecular Design and Engineering, Graduate School of Engineering, Nagoya University, Chikusa-ku, Nagoya 464-8603, Japan. E-mail: yashima@apchem.nagoya-u.ac.jp*

[b]*Venture Business Laboratory, Nagoya University, Chikusa-ku, Nagoya 464-8603, Japan*

† Electronic supplementary information (ESI) available: Experimental details and additional spectroscopic data. See DOI: 10.1039/c4sc02275k

monodentate phosphine ligands, such as (*R*)- or (*S*)-2-diphenylphosphino-2′-methoxy-1,1′-binaphthyl (MOP), coordinated to the Pt^{II} atom in the linkage[12] (Scheme 1A).[15]

We found that an optically-active double helix composed of two complementary strands bearing achiral amidine or carboxylic acid residues, linked through the Pt^{II}–acetylide complexes with (*R*)- or (*S*)-MOP or achiral triphenylphosphine (PPh_3) ligands, exhibited an inversion of the helicity in different solvents at low temperatures,[12] suggesting the dynamic nature of the Pt^{II}-linked double helix.[14k] The chiral and achiral monodentate phosphine ligands on the Pt^{II} atoms could be quantitatively replaced by an achiral diphosphine ligand, such as bis(diphenylphosphino)methane (DPPM), through the interstrand ligand-exchange reaction, resulting in the bridged double helix (right in Scheme 1A).[12] Interestingly, the bridged double helix, which no longer possessed any chiral components, except for helicity, maintained its preferred-handed helical conformation induced by the chiral MOP ligand for a long time period (over 100 days at 298 K). This enantiomerically-enriched double helix further catalyzed the asymmetric cyclopropanation of styrene with a high enantioselectivity (up to 85% enantiomeric excess) when complexed with Cu^{I} ions, thus providing the first asymmetric catalyst based on a unique bridged double-helical structure.[12]

It has been reported that the *trans*-Pt^{II}–acetylide complexes with PPh_3 ligands can be readily transformed into the *cis*-Pt^{II}–acetylides in the presence of chelating diphosphine ligands, such as *cis*-bis(diphenylphosphino)ethylene, cyclic diphosphines, and substituted diphosphinoethanes, by an intrastrand ligand exchange, whereas achiral 1,3-diphenylphosphinopropane (DPPPr) and chiral 2,4-bis(diphenylphosphino)pentane (DPPPe) produced dimeric *trans*-Pt^{II}–acetylide complexes bridged by the diphosphine ligands through the interstrand ligand exchange.[16,17]

Based on these results, together with our previous findings,[12] we anticipated that both the stability and helical handedness of the Pt^{II}-linked double helices could be enhanced and controlled using chiral chelating diphosphine ligands as cross-linkers

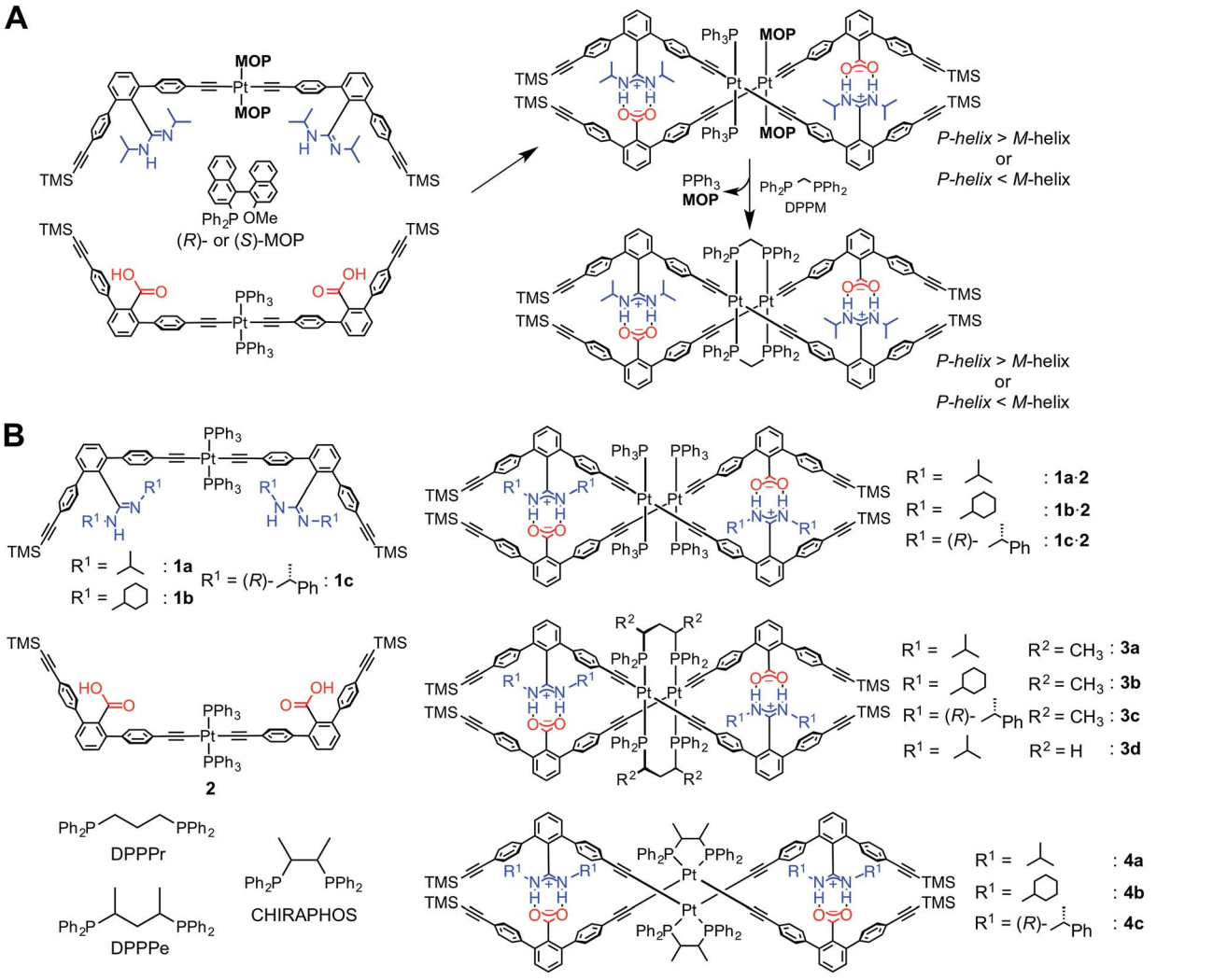

Scheme 1 Structures of the Pt^{II}–acetylide-linked amidine and carboxylic acid dimers (A and B), and their complementary duplexes before and after reactions with chiral (B) and achiral (A and B) diphosphines.

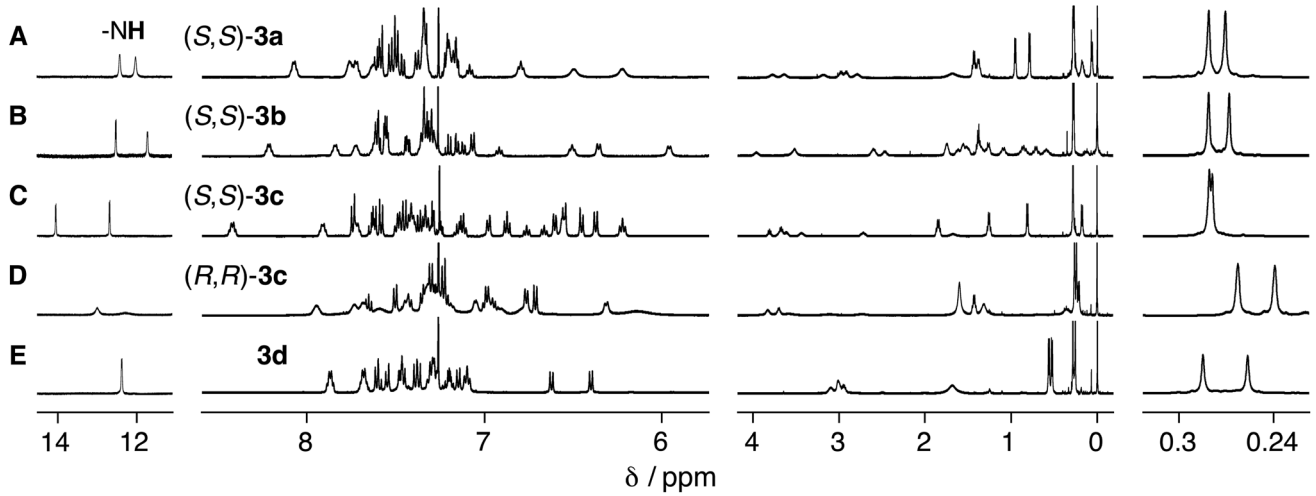

Fig. 1 Partial ^{1}H NMR (500 MHz, 2.0 mM) spectra of (A) (*S*,*S*)-**3a**, (B) (*S*,*S*)-**3b**, (C) (*S*,*S*)-**3c** (D) (*R*,*R*)-**3c**, and (E) **3d** in $CDCl_3$ at 25 °C.

during the ligand-exchange reactions. Although a variety of single-stranded helical polymers and foldamers have been developed, a "chiral cross-linking" approach has not yet been employed to control the helicity, except for a few examples.[9f,10f] To this end, we synthesized a series of Pt^{II}-linked dimer strands composed of chiral or achiral amidine (**1a–1c**) and achiral carboxylic acid dimer strands (**2**), and investigated the effects of chiral diphosphine ligands, such as (*S*,*S*)- or (*R*,*R*)-DPPPe and

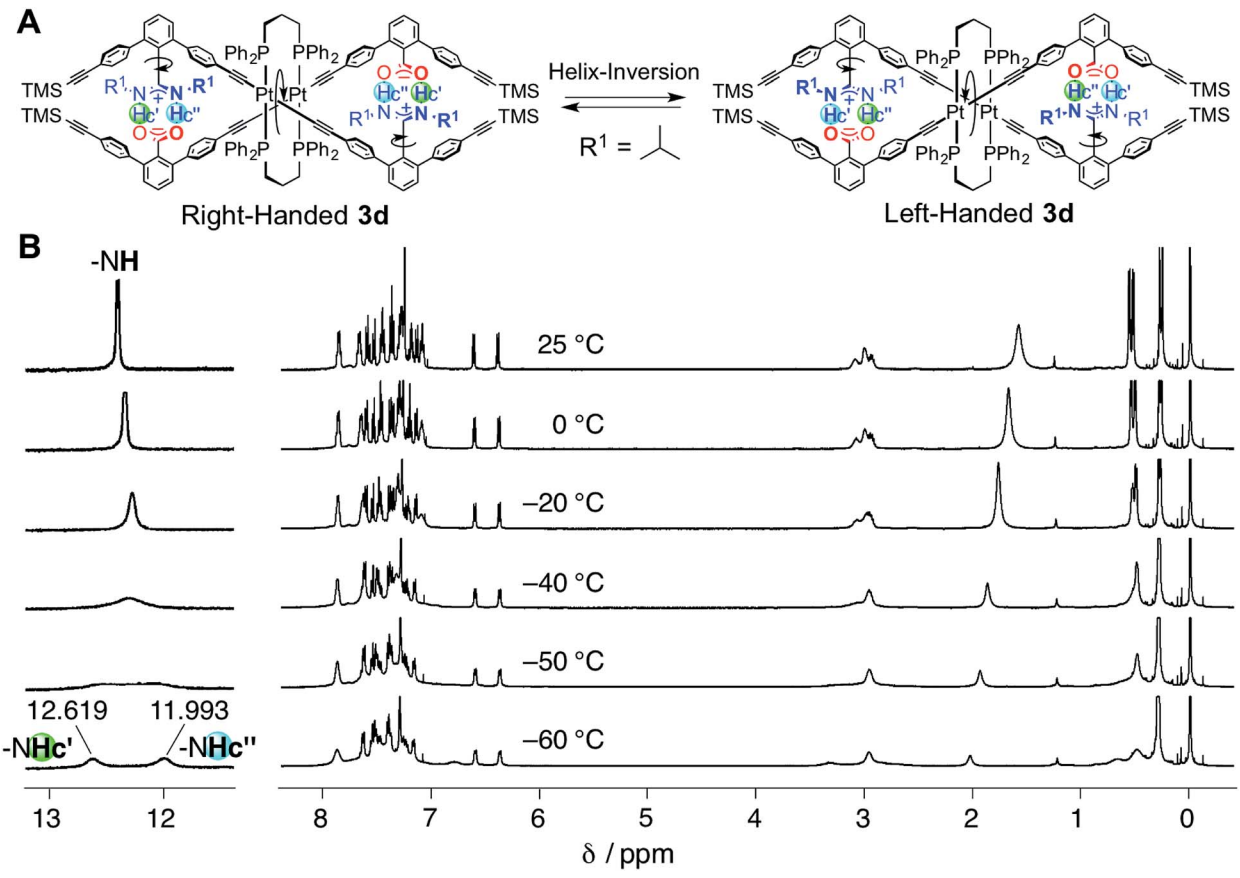

Fig. 2 (A) Schematic representation of the helix inversion of the duplex **3d**. The "outer" and "inner" N–H protons (Hc′ and Hc″) in the salt bridges become non-equivalent due to the interconvertible right- and left-handed double-helical structures under slow-exchange conditions. (B) Variable-temperature (from −60 to 25 °C) ^{1}H NMR (500 MHz, 2.0 mM) spectra of **3d** in $CDCl_3$ (the temperatures from −49 to −44 °C, used to estimate T_c, are also shown in Fig. S3†).

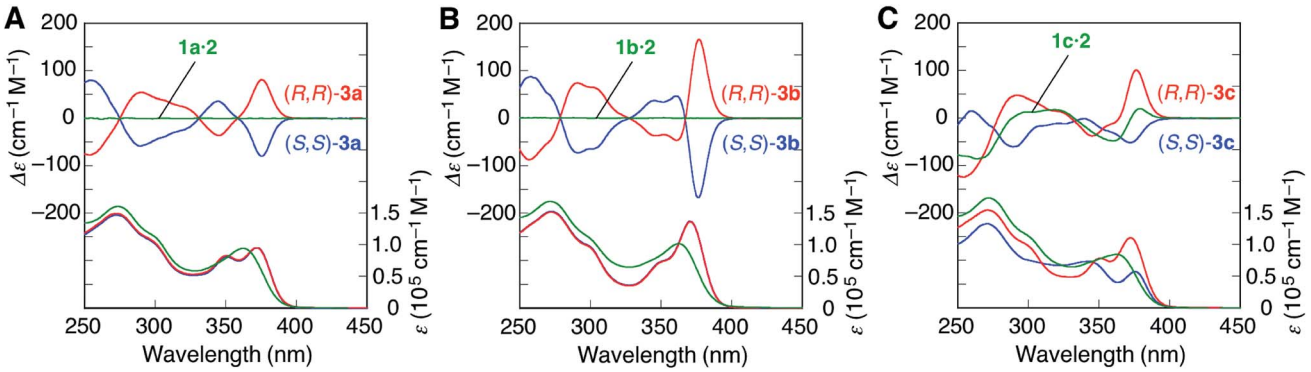

Fig. 3 CD and absorption spectra (0.1 mM) of (A) **1a**·**2**, (*S*,*S*)-**3a**, and (*R*,*R*)-**3a**, (B) **1b**·**2**, (*S*,*S*)-**3b**, and (*R*,*R*)-**3b**, and (C) **1c**·**2**, (*S*,*S*)-**3c**, and (*R*,*R*)-**3c** in $CHCl_3$ at 25 °C.

(*S*,*S*)- or (*R*,*R*)-2,3-bis(diphenylphosphino)butane (CHIRAPHOS), and substituents on the amidine residues. These included the effect of chirality on the structures, stabilities, and chiroptical properties of the double helices (**3**–**4**) resulting from the ligand-exchange reactions on the Pt^{II} atoms (Scheme 1B), measured using absorption, circular dichroism (CD), and ^1H and ^{31}P NMR spectroscopies. We also found that the ligand-exchange reaction on the Pt^{II} atoms with racemic DPPPe proceeded in a diastereoselective manner, producing the non-racemic bridged double helix, when a Pt^{II}-linked chiral amidine dimer (**1c**) and **2** were used as a precursor duplex.

Results and discussion

Synthesis and the ligand-exchange reaction

The achiral (**1a**)[12] and chiral ((*R*)-**1c**)[14b] amidine dimers and the achiral carboxylic acid dimer (**2**)[12] connected through the Pt^{II}–acetylide complex with two PPh_3 ligands, and their corresponding duplexes (**1a**·**2**,[12] and **1c**·**2**)[14b] were prepared according to previously reported methods (Scheme 1B). A novel achiral amidine dimer (**1b**) and its complementary duplex (**1b**·**2**) were also synthesized in a similar way.

The ligand-exchange reactions on the Pt^{II} atoms of the *trans*-Pt^{II} duplexes **1a**–**c**·**2** were carried out using 2 equiv. of the chiral diphosphines, (*S*,*S*)- or (*R*,*R*)-DPPPe and (*S*,*S*)- or (*R*,*R*)-CHIRAPHOS, and achiral DPPPr. The resulting double helices were purified by size-exclusion chromatography (SEC) and characterized and identified using ^1H and ^{31}P NMR spectroscopies, and elemental analyses or cold-spray ionization mass spectroscopy (CSI-MS) measurements (Fig. S1 and S2, and ESI†).

Effect of the chiral and achiral diphosphines on the duplex structures

The ligand-exchange reaction of the *trans*-Pt^{II} duplexes **1a**–**c**·**2** with a chiral diphosphine, (*S*,*S*)- or (*R*,*R*)-DPPPe (2 equiv.), gave the optically-active bridged double helices, (*S*,*S*)- and (*R*,*R*)-**3a**–**c**, respectively, while maintaining the *trans* geometry around the Pt^{II} center (Scheme 1B), as confirmed by the ^1H and ^{31}P NMR spectra (Fig. 1 and S1†).[18] The analogous achiral diphosphine, DPPPr, also produced the *trans*-Pt^{II}-bridged double helix (**3d**) (Scheme 1B), as supported by its ^{31}P NMR spectra (Fig. S1†).[18] These results indicated that the ligand exchange of **1a**–**c**·**2** with 1,3-diphosphine-based ligands (DPPPe and DPPPr) takes place *via* an interstrand fashion, thus producing the bridged double

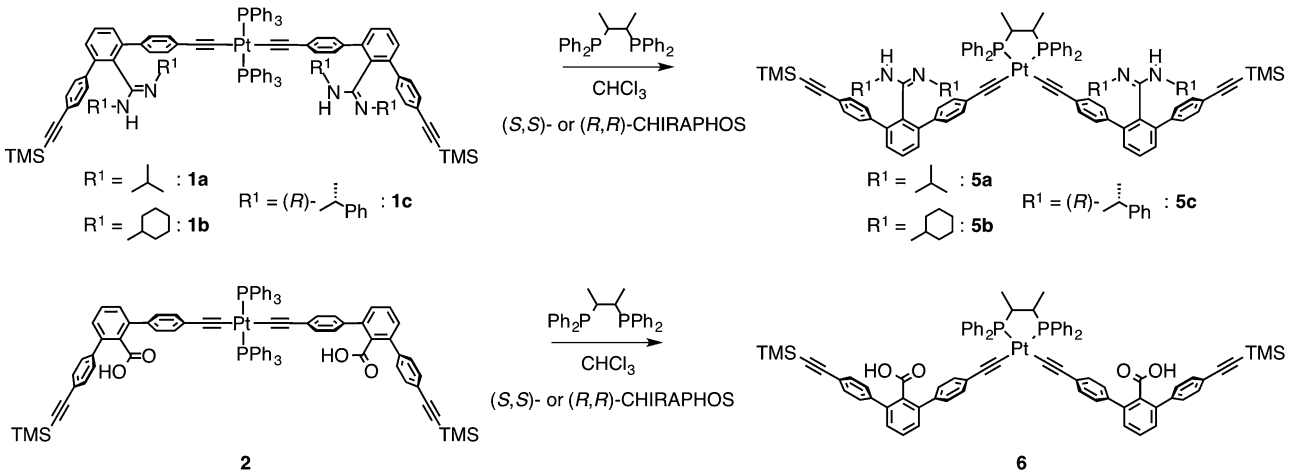

Scheme 2 Synthesis of the *cis*-Pt^{II}–acetylide-linked amidine (**5a**–**c**) and carboxylic acid (**6**) dimers with (*S*,*S*)- or (*R*,*R*)-CHIRAPHOS ligand.

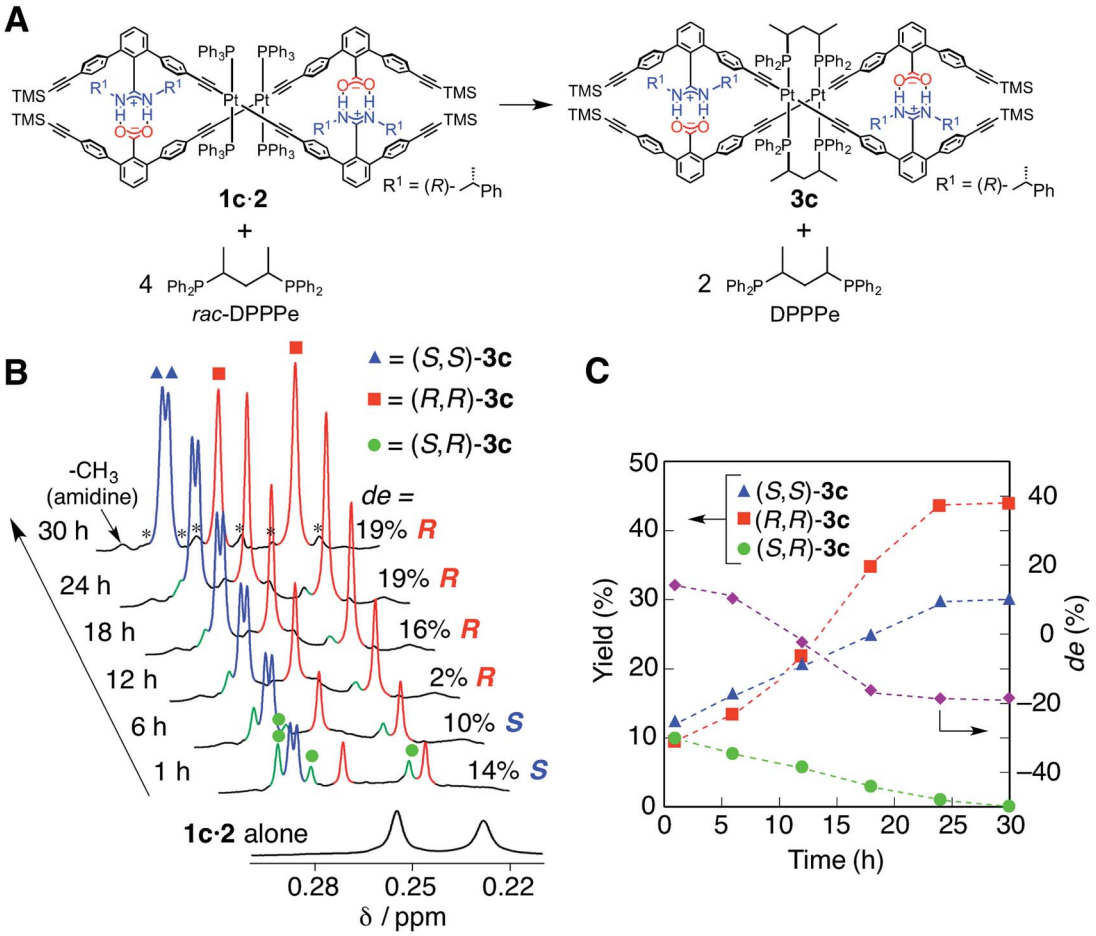

Fig. 4 (A) Interstrand ligand exchange of **1c·2** with 4 equiv. of *rac*-DPPPe. (B) Time-dependent ^{1}H NMR spectral changes of **1c·2** (TMS region) before and after the addition of 4 equiv. of *rac*-DPPPe in $CDCl_3$ at 25 °C; $[\mathbf{1c\cdot2}]_0 = 0.5$ mM, $[rac\text{-DPPPe}]_0 = 2.0$ mM. The ^{29}Si satellite peaks are marked with asterisks. (C) Plots of the yields and diastereomeric excess (de) of the resulting duplexes **3c** *versus* time. The yields were estimated using an internal standard (1,3,5-trioxane).

helices. However, treating the duplexes **1a–c·2** with 2 equiv. of (*S*,*S*)- or (*R*,*R*)-CHIRAPHOS led to the formation of the non-cross-linked duplexes **4a–c** whose ^{31}P NMR spectra were different from those of **3a–d** (Fig. S1†; see below for more details) (Scheme 1B).[19]

As previously reported,[14] the related complementary double helices, composed of chiral amidine and achiral carboxylic acid dimeric strands connected by various types of linkers including Pt^{II}–acetylide linkages, possess an excess of either a right- or left-handed double-helical structure. Therefore, the salt-bridged N–H protons (Hc′ and Hc″) exhibited in their ^{1}H NMR spectra two sets of non-equivalent signals around 12–14 ppm due to "outer" and "inner" N–H protons, as observed for the present optically-active **3a–c** (Fig. 1A–D), most likely derived from the preferred-handed double-helical structures as depicted in Fig. 2A.[14]

In contrast, the bridged duplex **3d** displayed a single set of sharp peaks including the salt-bridged N–H proton resonances that appeared as the equivalent doublet peak at 12.37 ppm in $CDCl_3$ at 25 °C (Fig. 1E). The bridged duplex **3d** was optically inactive, but existed as a racemic mixture of interconvertible right- and left-handed double helices; the rate of helix inversion that accompanied the C–C bond rotation between the amidine and *m*-terphenyl groups (Fig. 2A) may have been too fast on the present NMR time scale to detect the non-equivalent N–H protons at this temperature.[14k] We then measured the variable-temperature ^{1}H NMR spectra of **3d** in $CDCl_3$ to estimate its helix inversion barrier and also to evaluate the effect of the interstrand cross-linking on the thermodynamic stability of the duplex (Fig. 2B).

Upon cooling to lower temperatures, the N–H proton signals of **3d** gradually broadened and subsequently split into two sets of non-equivalent signals at −60 °C (Fig. 2B) *via* the coalescence temperature ($T_c = -46$ °C) (Fig. S3†). We noted that an analogous Pt^{II}–acetylide-linked double helix bearing the triethylphosphine (PEt_3) ligands instead of DPPPr did not show such nonequivalent signal splitting, even at −80 °C in CD_2Cl_2,[14k] indicating the significant enhancement of the stability of the duplex by the interstrand cross-link. The obtained T_c, along with the chemical shift difference between the split signals ($\Delta\nu = 313$ Hz), enables us to estimate that the free energy of activation for the helix inversion ($\Delta G^{\ddagger}$) of the duplex **3d** is 42.7 kJ

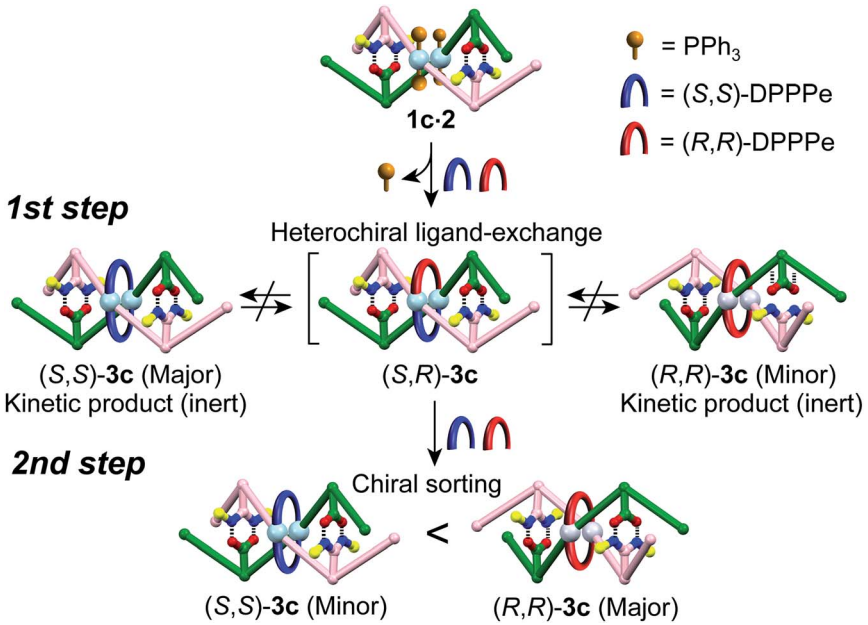

Fig. 5 Schematic representation of a proposed mechanism for the diastereoselective switching of **3c** during the interstrand ligand-exchange reaction with *rac*-DPPPe.

mol^{-1} at 25 °C, which corresponds to the lifetime of the one-handed helical state (τ) of 4.98×10^{-6} s. The $\Delta G^{\ddagger}$ value obtained for **3d** appears to be much higher than that for the Pt^{II}-linked duplex bearing the PEt_3 ligands,[14k] but lower than that of the bridged double helix by the DPPM ligands (Scheme 1A), because the enantiomerically-enriched DPPM-bridged double helix retains its optical activity for a long time.[12]

These results clearly indicated that the helix-inversion barrier, in other words, the stability of the bridged double-helical conformations, significantly depends on the structure of the chelating diphosphines, in particular, the length between the phosphorous atoms and the flexibility of the diphosphines, which determines the distance between the two Pt^{II} atoms on each complementary strand after the ligand exchange. In fact, the energy-minimized double-helical structure of **3d** (determined using the PM6 method[20] in MOPAC2012 (ref. 21)) revealed that the Pt–Pt distance (5.4 Å) is much longer than that of the DPPM-linked double helix (3.1 Å) in the crystalline state[12] (Fig. S4A†).

In contrast to **3d**, the amidinium N–H proton resonances in the ^{1}H NMR spectra of (*S*,*S*)-**3a** and -**3b** in $CDCl_3$ at 25 °C showed two sets of non-equivalent signals, even though the amidine groups are achiral (Fig. 1A and B), suggesting that these double helices probably adopt a preferred-handed double-helical structure induced by the chiral cross-linkers. The enantiomeric duplexes showed intense Cotton effects that are mirror images of each other (Fig. 3A and B).[22] In addition, the CD spectral patterns of (*S*,*S*)-**3a** and -**3b** are comparable to that of the diacetylene-connected dimeric duplex bearing the chiral amidine groups with an (*R*)-configuration, whose helical structure was determined to be right-handed by the single-crystal X-ray analysis.[14a]

The energy difference (ΔE) between the right- and left-handed double helices of (*S*,*S*)-**3a** was then estimated by semi-empirical molecular orbital (MO) calculations (using the PM6 method[20] in MOPAC2012 (ref. 21)), which revealed that the right-handed double-helical structure is 34.2 kJ mol^{-1} more stable than the other (Fig. S4B†), which is consistent with the preferred-handed helix sense predicted by its CD pattern.

Interestingly, the diastereomeric (*S*,*S*)- and (*R*,*R*)-**3c** duplexes with the same (*R*)-configuration at the amidine residues also exhibited mirror image-like CD spectra (Fig. 3C), suggesting that the helix sense of **3c** is predominantly governed by the chirality of the cross-linkers rather than the chirality of the amidine groups.[23] However, the CD and absorption intensities between the diastereomers of **3c** around 375 nm are significantly different from each other, probably due to the difference in the conformational flexibility around the Pt^{II}–phenylacetylide moieties, the absorption bands of which (metal-to-ligand charge transfer: MLCT) appear in this region.[24] In fact, the ^{1}H NMR spectrum of (*S*,*S*)-**3c** showed a series of sharp signals, including two sets of sharp doublet peaks assigned to the non-equivalent salt-bridged N–H protons at 14.00 and 12.29 ppm (Fig. 1C), while most of the proton signals, in particular, the N–H protons, of (*R*,*R*)-**3c** became considerably broadened (Fig. 1D).

The energy-minimized structures of the left-handed (*R*,*R*)-**3c** and right-handed (*S*,*S*)-**3c** duplexes suggest that the molecular motion of the (*R*,*R*)-**3c** duplex is highly restricted compared to the other due to the steric repulsion between the *m*-terphenyl groups and the bridged diphosphine ligands (Fig. S5†). The temperature-dependent CD and absorption spectral changes further support this speculation; the CD and absorption spectra of the (*R*,*R*)-**3c** hardly changed in the temperature range −10 to

50 °C, while the CD intensity of the (*S*,*S*)-**3c** increased with decreasing temperature (Fig. S6†).

It is noteworthy that all the bridged duplexes with chiral DPPPe ligands (**3a–c**) showed intense CD signals in $CHCl_3$ and even in dimethyl sulfoxide (DMSO) (Fig. S7†). In DMSO, the salt-bridge formation is strongly hampered,[14k] and therefore, the non-cross-linked **1c**·**2** duplex readily dissociates into each strand in DMSO, thus showing a very weak CD spectrum identical to that of the **1c** strand (Fig. S7E†) and indicating that the interstrand cross-linking remarkably stabilizes the complementary double helices.

The intrastrand ligand-exchange reaction

In contrast to the interstrand ligand-exchange reactions discussed above, the duplexes **1a**·**2**, **1b**·**2**, and **1c**·**2** were found to undergo ligand exchange *via* an intrastrand mechanism when 2 equiv. of (*S*,*S*)- or (*R*,*R*)-CHIRAPHOS were used as a chiral chelating diphosphine, leading to the formation of the non-cross-linked **4a–c** through the isomerization of the *trans*- to *cis*-Pt^{II}–acetylide moieties.[19] The structures were confirmed by ^{31}P NMR measurements, in which the $^1J_{P-Pt}$ coupling constants of **4a–c** were in the range of 2198–2249 Hz, that are consistent with the reported values for the *cis*-Pt^{II}–acetylide complexes with the phosphine ligands (Scheme 1B and Fig. S1†).[16b]

In order to further support the structural assignments, a series of model dimers, *cis*-Pt^{II}–acetylide-linked amidine (**5a–c**) and carboxylic acid (**6**) dimers with (*S*,*S*)- or (*R*,*R*)-CHIRAPHOS ligands, were prepared (Scheme 2) starting from **1a–c** and **2**.[14b,16,17] The ^1H NMR, CD, and absorption spectra of the model duplexes (*S*,*S*)-**5a**·**6**, (*S*,*S*)-**5b**·**6**, (*S*,*S*)-**5c**·**6**, and (*R*,*R*)-**5c**·**6** are almost identical to those of the (*S*,*S*)-**4a**, (*S*,*S*)-**4b**, (*S*,*S*)-**4c**, and (*R*,*R*)-**4c** duplexes, respectively (Fig. S8–S11†).[25]

Unlike in the case of the bridged **3a–c** duplexes, **4a–c** and their model duplexes (**5**·**6**) almost completely dissociated into corresponding single strands in DMSO, based on their CD spectra in DMSO (Fig. S12†),[14k] and most of the ^1H NMR signals of **4a–c** measured in $CDCl_3$ at 25 °C were highly broadened (Fig. S8A–S11A†) as anticipated because of their non-cross-linked structures. The amidinium N–H proton resonances of (*S*,*S*)-**4a** and -**4b** (Fig. S8A and S9A†) displayed an equivalent broad singlet peak (12.02 ppm), despite the N–H signals of (*S*,*S*)-**3a** and -**3b** showing non-equivalency (Fig. 1A and B). It seems likely that (*S*,*S*)-**4a** and -**4b** are in equilibrium between the single strands and the duplex, or adopt a double-helical structure without a helix-sense bias. Therefore, their CD intensities were much lower than those of the bridged duplexes **3a** and **3b** (Fig. 3 and S13†). This is probably due to conformational flexibility around the chiral phosphine moieties of **4a** and **4b**, resulting in an inefficient stereochemical communication between the chiral phosphine groups and the main chain. Unexpectedly, the N–H proton resonances of (*R*,*R*)-**4c** showed multiple N–H signals in $CDCl_3$ (Fig. S11A†), whereas those of (*S*,*S*)-**4c** exhibited two sets of non-equivalent signals (Fig. S10A†). The reason for this is not clear at present, but is considered to be due to the presence of two conformers that may slowly interconvert on the present NMR time scale *via* dissociation and association of the salt bridges for (*R*,*R*)-**4c**.[26]

The diastereoselective interstrand ligand-exchange reaction

The optically-active Pt^{II}-linked (*R*)-**1c**·**2** possesses an excess one-handed double-helical structure induced by the chiral amidine residues, and exhibited intense CD signals in the *m*-terphenyl chromophore region as well as in the Pt^{II}–acetylide complex region (*ca.* 330–400 nm) (Fig. 3C).[12,14b,14k] Therefore, we anticipated that the interstrand ligand-exchange reaction on the Pt^{II} atoms of the optically active **1c**·**2** using racemic DPPPe (*rac*-DPPPe) could diastereoselectively proceed, assisted by the one-handed double-helical structure of **1c**·**2**, thus selectively producing either the right- or left-handed bridged duplex **3c** (Fig. 4A). To this end, the optically-active **1c**·**2** was allowed to react with excess *rac*-DPPPe (4 equiv.) in $CDCl_3$ at 25 °C, and the reaction progress was monitored by ^1H NMR spectroscopy.

The ^1H NMR spectra (TMS region, Fig. 4B) of the mixtures after 1 h showed two distinct sets of signals derived from the amidine and carboxylic acid strands, namely the bridged duplexes (*S*,*S*)-**3c** (blue triangles) and (*R*,*R*)-**3c** (red squares) in addition to unknown signals (green circles), which gradually decreased with time and almost disappeared within 30 h (Fig. 4C).[27] We assigned this unknown product to the low-symmetric, heterochiral bridged duplex ((*S*,*R*)-**3c**) bearing both the (*S*,*S*)- and (*R*,*R*)-DPPPe ligands, that may be formed during the ligand-exchange reaction under kinetic control and which should be labile. This assignment was supported by the following facts: (1) the unknown signals remained even after 24 h when 2 equiv. of *rac*-DPPPe was added to a solution of **1c**·**2**, so that no further ligand exchange took place between the homochiral duplexes (*S*,*S*)- and (*R*,*R*)-**3c** once the DPPPe ligands were consumed (Fig. S14 and S15†); (2) a similar trend was observed for a mixture of (*S*,*S*)- and (*R*,*R*)-**3c** that is inert to the ligand-exchange reaction even in the presence of an excess amount of free ligands with the opposite configuration (2 equiv.) (Fig. S16†), leading to the conclusion that there is no ligand exchange among the three homo- and heterochiral bridged duplexes **3c** once formed under the present conditions (Fig. 5, 1st step).

The initial stage of the diastereoselective ligand-exchange reaction resulted in the formation of an excess of (*S*,*S*)-**3c** over (*R*,*R*)-3c in 14% diastereomeric excess (de) ((*S*,*S*)-rich) (Fig. 4B and C). Interestingly, as the reaction progressed, (*R*,*R*)-**3c** was preferentially formed, accompanied by a gradual decrease in the amount of (*S*,*R*)-**3c** with time, leading to reversed diastereoselectivity up to 19% de ((*R*,*R*)-rich) after 30 h (Fig. 4C).[28] This change in the diastereoselectivity could be explained as follows: the initial rate of formation of (*S*,*S*)-**3c** from the reaction of **1c**·**2** with enantiopure (*S*,*S*)-DPPPe is higher than that of (*R*,*R*)-**3c** from the reaction of **1c**·**2** with enantiopure (*R*,*R*)-DPPPe (Fig. S17†). As described above, the two homochiral double helices, (*S*,*S*)- and (*R*,*R*)-**3c**, are inert once formed by the ligand-exchange reaction, whereas the heterochiral (*S*,*R*)-**3c** is optically active and labile, thus, it is converted into either homochiral (*S*,*S*)- or (*R*,*R*)-**3c** in the presence of free DPPPe ligands. The

formation of (*R*,*R*)-**3c** is preferred to that of (*S*,*S*)-**3c** (Fig. 5, 2nd step).[29] Thus, the complete diastereoselective homochiral sorting eventually takes place under total kinetic control. The diastereoselectivity of *rac*-DPPPe was initially determined by a preferred-handed double helix assisted by the chiral amidine residues under kinetic control, while the overall diastereoselectivity was governed by the kinetically-formed (*S*,*R*)-**3c**.

Conclusions

In summary, we have successfully synthesized a series of novel Pt^{II}-linked double helices through inter- or intrastrand ligand-exchange reactions of the corresponding complementary duplexes using chiral and achiral diphosphines. The diphosphine structures significantly influenced the duplex structures; chiral and achiral 1,3-diphosphine-based ligands produced the *trans*-Pt^{II}-bridged double helices *via* an interstrand ligand exchange reaction, whereas a 1,2-diphosphine-based ligand gave non-cross-linked *cis*-Pt^{II}-linked duplexes through an intrastrand ligand exchange reaction. The former duplexes were quite stable even in DMSO due to the interstrand cross-link, while the latter duplexes readily dissociated into each strand in DMSO. When enantiomerically-pure 1,3-diphosphine-based ligands were used, optically-active *trans*-Pt^{II}-bridged double helices could be obtained; the helix sense was controlled by the chirality of the bridged diphosphines. Interestingly, the interstrand ligand exchange with racemic 1,3-diphosphine toward an optically-active Pt^{II}-linked duplex composed of a chiral amidine strand diastereoselectively proceeded, finally producing totally homochiral *trans*-Pt^{II}-bridged double helices *via* complete homochiral self-sorting.[30] The present findings will provide a versatile means for the rational design of functional double helix-based chiral materials for chiral recognition and also asymmetric catalysis[12] with high stability and selectivity. Further work along this line is currently ongoing in our laboratory.

Acknowledgements

This work was supported in part by Grant-in-Aid for Scientific Research (S) from the Japan Society for the Promotion of Science and by the Nanotechnology Platform Program (Molecule and Material Synthesis) of the Ministry of Education, Culture, Sports, Science and Technology, Japan. M. H. expresses her thanks for a JSPS Research Fellowship for Young Scientists (no. 10192).

Notes and references

1 For reviews on synthetic helical polymers, see: (*a*) M. M. Green, J.-W. Park, T. Sato, A. Teramoto, S. Lifson, R. L. B. Selinger and J. V. Selinger, *Angew. Chem., Int. Ed.*, 1999, **38**, 3138–3154; (*b*) M. Fujiki, *Macromol. Rapid Commun.*, 2001, **22**, 539–563; (*c*) T. Nakano and Y. Okamoto, *Chem. Rev.*, 2001, **101**, 4013–4038; (*d*) J. W. Y. Lam and B. Z. Tang, *Acc. Chem. Res.*, 2005, **38**, 745–754; (*e*) E. Yashima, K. Maeda and Y. Furusho, *Acc. Chem. Res.*, 2008, **41**, 1166–1180; (*f*) D. Pijper and B. L. Feringa, *Soft Matter*, 2008, **4**, 1349–1372; (*g*) E. Yashima, K. Maeda, H. Iida, Y. Furusho and K. Nagai, *Chem. Rev.*, 2009, **109**, 6102–6211; (*h*) E. Schwartz, M. Koepf, H. J. Kitto, R. J. M. Nolte and A. E. Rowan, *Polym. Chem.*, 2011, **2**, 33–47; (*i*) M. Shiotsuki, F. Sanda and T. Masuda, *Polym. Chem.*, 2011, **2**, 1044–1058.

2 For reviews on synthetic helical oligomers, see: (*a*) S. H. Gellman, *Acc. Chem. Res.*, 1998, **31**, 173–180; (*b*) D. J. Hill, M. J. Mio, R. B. Prince, T. S. Hughes and J. S. Moore, *Chem. Rev.*, 2001, **101**, 3893–4011; (*c*) I. Huc, *Eur. J. Org. Chem.*, 2004, 17–29; (*d*) D. Seebach, A. K. Beck and D. J. Bierbaum, *Chem. Biodiversity*, 2004, **1**, 1111–1239; (*e*) A. R. Sanford, K. Yamato, X. Yang, L. Yuan, Y. Han and B. Gong, *Eur. J. Biochem.*, 2004, **271**, 1416–1425; (*f*) S. Hecht and I. Huc, *Foldamers: Structure, Properties, and Applications*, Wiley-VCH, Weinheim, Germany, 2007; (*g*) Y. Inai, H. Komori and N. Ousaka, *Chem. Rec.*, 2007, **7**, 191–202; (*h*) I. Saraogi and A. D. Hamilton, *Chem. Soc. Rev.*, 2009, **38**, 1726–1743; (*i*) H. Juwarker and K.-S. Jeong, *Chem. Soc. Rev.*, 2010, **39**, 3664–3674; (*j*) G. Guichard and I. Huc, *Chem. Commun.*, 2011, **47**, 5933–5941; (*k*) D.-W. Zhang, X. Zhao, J.-L. Hou and Z.-T. Li, *Chem. Rev.*, 2012, **112**, 5271–5316.

3 For reviews on synthetic double helices, see: (*a*) E. C. Constable, *Tetrahedron*, 1992, **48**, 10013–10059; (*b*) J.-M. Lehn, *Supramolecular Chemistry: Concepts and Perspectives*, VCH, Weinheim, Germany, 1995; (*c*) C. Piguet, G. Bernardinelli and G. Hopfgartner, *Chem. Rev.*, 1997, **97**, 2005–2062; (*d*) M. Albrecht, *Chem. Rev.*, 2001, **101**, 3457–3497; (*e*) Y. Furusho and E. Yashima, *Chem. Rec.*, 2007, **7**, 1–11; (*f*) R. Amemiya and M. Yamaguchi, *Org. Biomol. Chem.*, 2008, **6**, 26–35; (*g*) Y. Furusho and E. Yashima, *J. Polym. Sci., Part A: Polym. Chem.*, 2009, **47**, 5195–5207; (*h*) D. Haldar and C. Schmuck, *Chem. Soc. Rev.*, 2009, **38**, 363–371; (*i*) Y. Furusho and E. Yashima, *Macromol. Rapid Commun.*, 2011, **32**, 136–146; (*j*) S. E. Howson and P. Scott, *Dalton Trans.*, 2011, **40**, 10268–10277.

4 For reviews and leading examples of PNA, see: (*a*) P. E. Nielsen, M. Egholm, R. H. Berg and O. Buchardt, *Science*, 1991, **254**, 1497–1500; (*b*) P. Wittung, P. E. Nielsen, O. Buchardt, M. Egholm and B. Norden, *Nature*, 1994, **368**, 561–563; (*c*) P. E. Nielsen, *Acc. Chem. Res.*, 1999, **32**, 624–630; (*d*) F. Totsingan, V. Jain, W. C. Bracken, A. Faccini, T. Tedeschi, R. Marchelli, R. Corradini, N. R. Kallenbach and M. M. Green, *Macromolecules*, 2010, **43**, 2692–2703.

5 For examples of helicates, see: (*a*) C. J. Carrano and K. N. Raymond, *J. Am. Chem. Soc.*, 1978, **100**, 5371–5374; (*b*) J.-M. Lehn, A. Rigault, J. Siegel, J. Harrowfield, B. Chevrier and D. Moras, *Proc. Natl. Acad. Sci. U. S. A.*, 1987, **84**, 2565–2569; (*c*) U. Koert, M. M. Harding and J.-M. Lehn, *Nature*, 1990, **346**, 339–342; (*d*) C. R. Woods, M. Benaglia, F. Cozzi and J. S. Siegel, *Angew. Chem., Int. Ed. Engl.*, 1996, **35**, 1830–1833; (*e*) H. Katagiri, T. Miyagawa, Y. Furusho and E. Yashima, *Angew. Chem., Int. Ed.*, 2006, **45**, 1741–1744; (*f*) K. Miwa, Y. Furusho and E. Yashima, *Nat. Chem.*, 2010, **2**, 444–449; (*g*) Y. Furusho, K. Miwa,

R. Asai and E. Yashima, *Chem.–Eur. J.*, 2011, **17**, 13954–13957; (*h*) M. Albrecht, E. Isaak, M. Baumert, V. Gossen, G. Raabe and R. Fröhlich, *Angew. Chem., Int. Ed.*, 2011, **50**, 2850–2853; (*i*) S. E. Howson, A. Bolhuis, V. Brabec, G. J. Clarkson, J. Malina, A. Rodger and P. Scott, *Nat. Chem.*, 2012, **4**, 31–36; (*j*) X. de Hatten, D. Asil, R. H. Friend and J. R. Nitschke, *J. Am. Chem. Soc.*, 2012, **134**, 19170–19178; (*k*) S. Yamamoto, H. Iida and E. Yashima, *Angew. Chem., Int. Ed.*, 2013, **52**, 6849–6853.

6 (*a*) V. Berl, I. Huc, R. G. Khoury, M. J. Krische and J.-M. Lehn, *Nature*, 2000, **407**, 720–723; (*b*) D. Haldar, H. Jiang, J.-M. Léger and I. Huc, *Angew. Chem., Int. Ed.*, 2006, **45**, 5483–5486; (*c*) Q. Gan, C. Bao, B. Kauffmann, A. Grelard, J. Xiang, S. Liu, I. Huc and H. Jiang, *Angew. Chem., Int. Ed.*, 2008, **47**, 1715–1718; (*d*) E. Berni, J. Garric, C. Lamit, B. Kauffmann, J.-M. Léger and I. Huc, *Chem. Commun.*, 2008, 1968–1970; (*e*) Q. Gan, Y. Ferrand, N. Chandramouli, B. Kauffmann, C. Aube, D. Dubreuil and I. Huc, *J. Am. Chem. Soc.*, 2012, **134**, 15656–15659.

7 For examples of the double-helix formation through hydrogen bonds with ions, see: (*a*) J. Sánchez-Quesada, C. Seel, P. Prados, J. de Mendoza, I. Dalcol and E. Giralt, *J. Am. Chem. Soc.*, 1996, **118**, 277–278; (*b*) J. Keegan, P. E. Kruger, M. Nieuwenhuyzen, J. O'Brien and N. Martin, *Chem. Commun.*, 2001, 2192–2193; (*c*) S. J. Coles, J. G. Frey, P. A. Gale, M. B. Hursthouse, M. E. Light, K. Navakhun and G. L. Thomas, *Chem. Commun.*, 2003, 568–569; (*d*) T. Sugimoto, T. Suzuki, S. Shinkai and K. Sada, *J. Am. Chem. Soc.*, 2007, **129**, 270–271; (*e*) H.-J. Kim, E. Lee, M. G. Kim, M.-C. Kim, M. Lee and E. Sim, *Chem.–Eur. J.*, 2008, **14**, 3883–3888; (*f*) Y. Haketa and H. Maeda, *Chem.–Eur. J.*, 2011, **17**, 1485–1492; (*g*) Y. Hua, Y. Liu, C.-H. Chen and A. H. Flood, *J. Am. Chem. Soc.*, 2013, **135**, 14401–14412.

8 For examples of the double-helix formation in water, see: (*a*) H. Goto, H. Katagiri, Y. Furusho and E. Yashima, *J. Am. Chem. Soc.*, 2006, **128**, 7176–7178; (*b*) H. Goto, Y. Furusho and E. Yashima, *J. Am. Chem. Soc.*, 2007, **129**, 9168–9174; (*c*) H. Goto, Y. Furusho and E. Yashima, *J. Am. Chem. Soc.*, 2007, **129**, 109–112; (*d*) H. Goto, Y. Furusho, K. Miwa and E. Yashima, *J. Am. Chem. Soc.*, 2009, **131**, 4710–4719.

9 For examples of intramolecularly cross-linked synthetic (single-stranded) helices, see: (*a*) S. Hecht and A. Khan, *Angew. Chem., Int. Ed.*, 2003, **42**, 6021–6024; (*b*) K. Maeda, H. Mochizuki, M. Watanabe and E. Yashima, *J. Am. Chem. Soc.*, 2006, **128**, 7639–7650; (*c*) Y. E. Bergman, M. P. D. Borgo, R. D. Gopalan, S. Jalal, S. E. Unabia, M. Ciampini, D. J. Clayton, J. M. Fletcher, R. J. Mulder, J. A. Wilce, M.-I. Aguilar and P. Perlmutter, *Org. Lett.*, 2009, **11**, 4438–4440; (*d*) R. A. Smaldone, E.-C. Lin and J. S. Moore, *J. Polym. Sci., Part A: Polym. Chem.*, 2010, **48**, 927–935; (*e*) S. Takashima, H. Abe and M. Inouye, *Chem. Commun.*, 2012, **48**, 3330–3332; (*f*) N. Fuentes, A. Martin-Lasanta, L. A. de Cienfuegos, R. Robles, D. Choquesillo-Lazarte, J. M. García-Ruiz, L. Martínez-Fernández, I. Corral, M. Ribagorda, A. J. Mota, D. J. Cárdenas, M. C. Carreño and J. M. Cuerva, *Angew. Chem., Int. Ed.*, 2012, **51**, 13036–13040.

10 For examples of intramolecularly cross-linked helical oligopeptides, see: (*a*) H. E. Blackwell and R. H. Grubbs, *Angew. Chem., Int. Ed.*, 1998, **37**, 3281–3284; (*b*) J. R. Kumita, O. S. Smart and G. A. Woolley, *Proc. Natl. Acad. Sci. U. S. A.*, 2000, **97**, 3803–3808; (*c*) D. G. Flint, J. R. Kumita, O. S. Smart and G. A. Woolley, *Chem. Biol.*, 2002, **9**, 391–397; (*d*) L. D. Walensky, A. L. Kung, I. Escher, T. J. Malia, S. Barbuto, R. D. Wright, G. Wagner, G. L. Verdine and S. J. Korsmeyer, *Science*, 2004, **305**, 466–470; (*e*) A. K. Boal, I. Guryanov, A. Moretto, M. Crisma, E. L. Lanni, C. Toniolo, R. H. Grubbs and D. J. O'Leary, *J. Am. Chem. Soc.*, 2007, **129**, 6986–6987; (*f*) N. Ousaka, T. Sato and R. Kuroda, *J. Am. Chem. Soc.*, 2009, **131**, 3820–3821.

11 For reviews, see: (*a*) M. L. G. Dronkert and R. Kanaar, *Mutat. Res.*, 2001, **486**, 217–247; (*b*) D. M. Noll, T. M. Mason and P. S. Miller, *Chem. Rev.*, 2006, **106**, 277–301; (*c*) A. J. Deans and S. C. West, *Nat. Rev. Cancer*, 2011, **11**, 467–480; (*d*) L. Brulikova, J. Hlavac and P. Hradil, *Curr. Med. Chem.*, 2012, **19**, 364–385.

12 T. Hasegawa, H. Goto, Y. Furusho, H. Katagiri and E. Yashima, *Angew. Chem., Int. Ed.*, 2007, **46**, 5885–5888. Double-stranded helicates were used as precursors to produce topologically unique [2]catenanes and molecular knots after specific interstrand and intrastrand cross-linking at both ends followed by demetallation.[13] Obviously, the double helix stability of the stapled helicates was remarkably enhanced.

13 For leading examples of stapled double-stranded helicates, see: (*a*) C. O. Dietrich-Buchecker and J.-P. Sauvage, *Angew. Chem., Int. Ed. Engl.*, 1989, **28**, 189–192; (*b*) C. O. Dietrich-Buchecker, J. Guilhem, C. Pascard and J.-P. Sauvage, *Angew. Chem., Int. Ed. Engl.*, 1990, **29**, 1154–1156; (*c*) *Molecular Catenanes, Rotaxanes and Knots*, ed. J.-P. Sauvage and C. O. Dietrich-Buchecker, Wiley-VCH, Weinheim, 1999.

14 For examples of complementary double helices based on amidinium–carboxylate salt bridges, see: (*a*) Y. Tanaka, H. Katagiri, Y. Furusho and E. Yashima, *Angew. Chem., Int. Ed.*, 2005, **44**, 3867–3870; (*b*) Y. Furusho, Y. Tanaka and E. Yashima, *Org. Lett.*, 2006, **8**, 2583–2586; (*c*) M. Ikeda, Y. Tanaka, T. Hasegawa, Y. Furusho and E. Yashima, *J. Am. Chem. Soc.*, 2006, **128**, 6806–6807; (*d*) Y. Furusho, Y. Tanaka, T. Maeda, M. Ikeda and E. Yashima, *Chem. Commun.*, 2007, 3174–3176; (*e*) H. Ito, Y. Furusho, T. Hasegawa and E. Yashima, *J. Am. Chem. Soc.*, 2008, **130**, 14008–14015; (*f*) T. Maeda, Y. Furusho, S.-i. Sakurai, J. Kumaki, K. Okoshi and E. Yashima, *J. Am. Chem. Soc.*, 2008, **130**, 7938–7945; (*g*) H. Iida, M. Shimoyama, Y. Furusho and E. Yashima, *J. Org. Chem.*, 2010, **75**, 417–423; (*h*) H. Yamada, Y. Furusho, H. Ito and E. Yashima, *Chem. Commun.*, 2010, **46**, 3487–3489; (*i*) H. Ito, M. Ikeda, T. Hasegawa, Y. Furusho and E. Yashima, *J. Am. Chem. Soc.*, 2011, **133**, 3419–3432; (*j*) H. Yamada, Y. Furusho and E. Yashima, *J. Am. Chem. Soc.*, 2012, **134**, 7250–7253; (*k*) H. Yamada, Z.-Q. Wu, Y. Furusho and E. Yashima, *J. Am. Chem. Soc.*, 2012, **134**, 9506–9520.

15 Metal–acetylide complexes, such as Pt^{II}–acetylide, have been recognized as useful building blocks to construct well-defined supramolecular architectures because of their well-defined geometry along with their synthetic accessibility, see: (*a*) P. J. Stang and B. Olenyuk, *Acc. Chem. Res.*, 1997, **30**, 502–518; (*b*) V. W.-W. Yam, *Acc. Chem. Res.*, 2002, **35**, 555–563; (*c*) K. Onitsuka and S. Takahashi, *Top. Curr. Chem.*, 2003, **228**, 39–63; (*d*) S. Szafert and J. A. Gladysz, *Chem. Rev.*, 2006, **106**, PR1–PR33; (*e*) S. Y.-L. Leung, A. Y.-Y. Tam, C.-H. Tao, H. S. Chow and V. W.-W. Yam, *J. Am. Chem. Soc.*, 2012, **134**, 1047–1056.

16 (*a*) G. R. Owen, F. Hampel and J. A. Gladysz, *Organometallics*, 2004, **23**, 5893–5895; (*b*) A. L. Sadowy, M. J. Ferguson, R. McDonald and R. R. Tykwinski, *Organometallics*, 2008, **27**, 6321–6325.

17 For other examples of ligand-exchange reactions at a Pt^{II}–acetylide center, see: (*a*) K. Campbell, R. McDonald, M. J. Ferguson and R. R. Tykwinski, *J. Organomet. Chem.*, 2003, **683**, 379–387; (*b*) K. Campbell, C. A. Johnson II, R. McDonald, M. J. Ferguson, M. M. Haley and R. R. Tykwinski, *Angew. Chem., Int. Ed.*, 2004, **43**, 5967–5971; (*c*) J. Stahl, W. Mohr, L. de Quadras, T. B. Peters, J. C. Bohling, J. M. Martín-Alvarez, G. R. Owen, F. Hampel and J. A. Gladysz, *J. Am. Chem. Soc.*, 2007, **129**, 8282–8295; see also ref. 12 and 14*b*.

18 The $^{1}J_{P-Pt}$ coupling constants of the bridged double helices in the range 2545–2663 Hz are consistent with the reported values for the *trans*-Pt^{II}–acetylide complexes with phosphine ligands.[16b]

19 Tykwinski and coworkers reported that the *trans*-Pt^{II}–alkenyl complexes with PPh_3 ligands could be smoothly transformed into the corresponding *cis*-form *via* a ligand-exchange reaction with CHIRAPHOS or *cis*-bis(diphenylphosphino) ethylene.[14b,17a,b]

20 J. J. P. Stewart, *J. Mol. Model.*, 2007, **13**, 1173–1213.

21 J. J. P. Stewart, *MOPAC2012, Stewart Computational Chemistry*, Colorado Springs, CO, USA, http://openmopac.net/, 2012.

22 The CD and absorption intensities of **3a** around 375 nm are smaller than those of **3b**, which may be attributed to a conformational flexibility arising from the less bulky amidine substituents of **3a**, compared to **3b**.

23 The right- and left-handed double-helical structures of (*S*,*S*)-**3c** and (*R*,*R*)-**3c** are 53.8 and 18.5 kJ mol^{-1} more stable than the corresponding opposite-handed duplexes, respectively, estimated by semi-empirical MO calculations (using the PM6 method[20] in MOPAC2012 (ref. 21)) (Fig. S4C and D†).

24 For discussions on the MLCT band in the Pt^{II}–acetylide complexes, see: (*a*) M. S. Khan, A. K. Kakkar, N. J. Long, J. Lewis, P. Raithby, P. Nguyen, T. B. Marder, F. Wittmann and R. H. Friend, *J. Mater. Chem.*, 1994, **4**, 1227–1232; (*b*) S. Takahashi, K. Onitsuka and F. Takei, *Macromol. Symp.*, 2000, **156**, 69–77; (*c*) R. D'Amato, A. Furlani, M. Colapietro, G. Portalone, M. Casalboni, M. Falconieri and M. V Russo, *J. Organomet. Chem.*, 2001, **627**, 13–22; (*d*) R. Saha, M. A. Qaium, D. Debnath, M. Younus, N. Chawdhury, N. Sultana, G. Kociok-Köhn, L.-L. Ooi, P. R. Raithby and M. Kijima, *Dalton Trans.*, 2005, 2760–2765.

25 It should be noted that the absorption band around 375 nm observed in **3a–c** with the *trans*-Pt^{II} geometry completely disappeared in the non-cross-linked *cis*-Pt^{II}–**4a–c** and their model duplexes **5a–c**·**6** (Fig. S8–S11†).[14b]

26 The rate of chain exchange between the dimeric strands in the related Pt^{II}-linked duplexes was reported to be much slower than the NMR time scale.[14k]

27 The relatively lower yields of **3c** during the initial stage of the ligand-exchange reaction may be due to imperfect bridging by DPPPe, resulting in the formation of complicated intermediates, such as duplexes bearing non-bridged DPPPe and PPh_3 ligands with different molar ratios, the signals of which would be highly broad. In fact, the TMS signals due to the **1c**·**2** (0.25 and 0.23 ppm) completely disappeared within 1 h (Fig. 4B).

28 A similar diastereoselectivity switching has been observed in the template synthesis of complementary double helices through the formation of dynamic-covalent imine bonds.[14j]

29 The diastereoselective ligand exchange of heterochiral (*S*,*R*)-**3c** toward (*S*,*S*)- and (*R*,*R*)-DPPPe was investigated as follows (Fig. S18†); first **1c**·**2** was allowed to react with 2 equiv. of *rac*-DPPPe to form unreactive homochiral (*S*,*S*)- and (*R*,*R*)-**3c** ((*S*,*S*) rich) as well as reactive (*S*,*R*)-**3c**. Upon the further addition of 2 equiv. of *rac*-DPPPe, the (*S*,*R*)-**3c** preferentially reacted with (*R*,*R*)-DPPPe over the antipode (*S*,*S*)-DPPPe, thus producing totally homochiral **3c** slightly rich in the (*R*,*R*)-**3c** duplex, which clearly revealed the (*R*,*R*)-selectivity of the heterochiral (*S*,*R*)-**3c**, although its diastereoselectivity was not high.

30 For reviews, see: (*a*) C. Maeda, T. Kamada, N. Aratani and A. Osuka, *Coord. Chem. Rev.*, 2007, **251**, 2743–2752; (*b*) M. M. Safont-Sempere, G. Fernández and F. Würthner, *Chem. Rev.*, 2011, **111**, 5784–5814; for selected examples of homochiral self-sorting in metallo-supramolecular assemblies, see: (*c*) M. A. Masood, E. J. Enemark and T. D. P. Stack, *Angew. Chem., Int. Ed.*, 1998, **37**, 928–932; (*d*) S. G. Telfer, T. Sato and R. Kuroda, *Angew. Chem., Int. Ed.*, 2004, **43**, 581–584; (*e*) M. Hutin, C. J. Cramer, L. Gagliardi, A. R. M. Shahi, G. Bernardinelli, R. Cerny and J. R. Nitschke, *J. Am. Chem. Soc.*, 2007, **129**, 8774–8780; (*f*) F. Rodler, W. Sicking and C. Schmuck, *Chem. Commun.*, 2011, **47**, 7953–7955; (*g*) C. Guetz, R. Hovorka, C. Klein, Q.-Q. Jiang, C. Bannwarth, M. Engeser, C. Schmuck, W. Assenmacher, W. Mader, F. Topic, K. Rissanen, S. Grimme and A. Lützen, *Angew. Chem., Int. Ed.*, 2014, **53**, 1693–1698.